JTTEE5 19:358–367
DOI: 10.1007/s11666-009-9387-1
1059-9630/$19.00 © ASM International

Wear and Corrosion Behavior of HVOF-Sprayed WC-CoCr Coatings on Al Alloys

M. Barletta, G. Bolelli, B. Bonferroni, and L. Lusvarghi

(Submitted April 24, 2009; in revised form August 5, 2009)

WC-CoCr coatings were HVOF-sprayed onto an AA6082T6 substrate. Thickness values between 50 and 150 μm were produced by stepwise increase of the number of torch scans. This increase made the coatings not only thicker but also denser. This was due both to peening effects and by modifications to the splat formation mechanism, investigated by focused ion beam technique. Thanks to such densification, the hardness, the wear and impact resistance, and the corrosion protectiveness of the layers increased with the number of torch scans. The largest improvement occurred from 2 to 3 torch scans. These coatings were also compared to anodized films: cermets had superior wear and impact resistance but offered less corrosion protection.

Keywords cermet coatings, corrosion resistance, HVOF, impact resistance, light alloys, sliding wear

1. Introduction

Light alloys (e.g., Al alloys) find increasingly large industrial use, in accordance to their high strength-to-density ratio and elastic modulus-to-density ratio (Ref 1). These alloys, however, have poor tribological behavior (Ref 2) and (depending on their composition) can be prone to localized corrosion (e.g., pitting) in some particularly aggressive environments (like seacoast atmosphere) (Ref 3, 4). To prevent these drawbacks, protective coatings or surface treatments are often employed.

Of the various surface treatments available for Al alloys, anodization ones are the most common (Ref 3). Conventional anodization treatments, carried out in a sulfuric or chromic acid bath at about 50 °C, produce a very thin and dense barrier layer with a much thicker porous layer on top of it. These pores are usually sealed by a treatment in hot water or by a lower temperature treatment in aqueous solutions containing suitable salts (often including Ni^{2+} and F^{-} ions) to enhance the corrosion protectiveness: during these treatments, some Al_2O_3 from the anodized film is dissolved and aluminum hydroxides (pseudo-bohemite) or Al-Ni-F hydroxides precipitate inside the pores. The pores are therefore closed, but the layer's hardness is somewhat impaired (Ref 3, 5). Alternatively, low-temperature (≤5 °C) hard anodizing treatments produce entirely dense layers, needing no sealing, so that optimized protection against wear is provided (Ref 3, 5).

Anodized films offer interesting properties but they are intrinsically quite brittle, have limited thickness, and require long processing times (several hours) (Ref 3, 5); additionally, they require a careful surface pretreatment and their outcome is strongly dependent on the alloy composition (Ref 3, 5, 6).

Thermal spraying technologies, in contrast, are less sensitive to the nature of the substrate, they only require a grit-blasting pretreatment, and they provide a flexible choice of coating thickness and of coating material (Ref 7). Specifically, dense HVOF-sprayed WC-CoCr cermets combine high hardness to satisfactory toughness and good corrosion resistance (Ref 8, 9). Research studies concerning WC-based HVOF coatings on light alloys are being carried out (Ref 2, 4, 10-12), but they are not very numerous.

Specifically, the above-mentioned literatures have not considered yet the effect of the coating thickness on its behavior: in a very thin coating, the contact stresses significantly affect the substrate, which may yield if it possesses low hardness (as is the case for Al alloys). Stress concentrations at the coating-substrate interface may then lead to premature failure of the system. On the other hand, producing a thinner coating would reduce the processing time and consumption of gas and powder.

This article is an invited paper selected from presentations at the 2009 International Thermal Spray Conference and has been expanded from the original presentation. It is simultaneously published in *Expanding Thermal Spray Performance to New Markets and Applications: Proceedings of the 2009 International Thermal Spray Conference*, Las Vegas, Nevada, USA, May 4-7, 2009, Basil R. Marple, Margaret M. Hyland, Yuk-Chiu Lau, Chang-Jiu Li, Rogerio S. Lima, and Ghislain Montavon, Ed., ASM International, Materials Park, OH, 2009.

M. Barletta, Department of Mechanical Engineering, University of Rome "Tor Vergata", Via del Politecnico 1, 00133 Rome, Italy; and **G. Bolelli, B. Bonferroni,** and **L. Lusvarghi**, Department of Materials and Environmental Engineering, University of Modena and Reggio Emilia, Via Vignolese 905, 41100 Modena, MO, Italy. Contact e-mail: luca.lusvarghi@unimore.it.

The best compromise should be sought for: the aim of this research is to assess the effect of the thickness on the mechanical properties, the tribological behavior, and the corrosion resistance of WC-CoCr coatings, deposited on an Al alloy by HVOF spraying using different numbers of torch scans. Their performances are also compared to those of anodized films.

2. Experimental

A commercially available WC-10%Co-4%Cr powder (Praxair 1350VM, −45 + 15 μm) was HVOF-sprayed onto grit-blasted Al alloy 6082-T6 plates of 80 × 80 × 8 mm^3 size. Grit-blasting was carried out using a manual blasting gun, positioned perpendicularly to the substrate surface, held at a distance of ~10 to 15 cm and operated at a pressure of 2 bar. Angular alumina powder was used as abrasive medium; specifically, a 50-50% mixture of 20 grit (Metcolite-C, Sulzer Metco, Winterthur, Switzerland) and 24 grit particles (Metcolite-F, Sulzer Metco) was adopted.

The HVOF spraying parameters, selected based on previous experience, are summarized in Table 1.

Coatings with increasing thickness were produced by performing a total of 2, 3, 4, and 5 complete torch scans in front of the substrate. Single splats were also collected onto ground Al and carbon steel plates, using the same deposition parameters as in Table 1, but greater traverse speed.

Other Al plates (not HVOF coated) were polished to $R_a \approx 0.02$ μm and anodized. Half of these plates were anodized according to a conventional process, performed at 50 °C in a sulfuric acid-based bath, and were subsequently sealed at room temperature in a water-based solution containing Ni^{2+} and F^- ions. The other half was subjected to a hard anodization process performed at 2 °C in a sulfuric acid-based bath. These processes were carried out in an industrial anodization plant, using proprietary process parameters.

Table 1 HVOF parameters (torch: Praxair-Tafa JP5000)

Barrel length, mm	152.4
O_2 flow rate, SL/min	873
Kerosene flow rate, L/min	0.379
Carrier gas flow rate, SL/min	11
Powder feed rate, g/min	98
Stand-off distance, mm	380
Torch traverse speed, mm/s	500
Interpass spacing, mm	3

On the polished cross-sections of the coatings, scanning electron microscopy (SEM: FEI XL30) and Vickers microindentation (Micro-Combi Tester, CSM Instruments: 1 N indentation load) were performed. The coatings' porosity was assessed by image analysis (ImageJ 1.37). Ball-on-disk tribological tests (Pin-on-Disk Tribometer, CSM Instruments) were performed on polished ($R_a \approx 0.02$ μm) cermet coatings and on the anodized layers, using 3 mm diameter WC-6%Co balls as counterparts. Test conditions include 10 N normal load, 0.20 m/s relative sliding speed, 5000 m overall sliding distance, 21 °C temperature, and 56% relative humidity. The sample wear rate was measured by optical confocal profilometry (Conscan Profilometer, CSM Instruments); the wear scars were observed by SEM.

Cyclic impact tests were conducted on WC-CoCr coatings and on anodized films, using the apparatus schematically shown in Fig. 1. The sample (label 1) was clamped onto the base of the instrument (label 4) and a 39 mm diameter X200Cr13 steel ball (label 2), attached to a holder (label 3) sliding along two vertical guides (label 5), was laid onto its surface. The ball + holder system (whose total mass was ~1.2 kg) was raised using permanent magnets (labels 7 and 8) attached to an electric motor, until it reached the bar (label 6) which defines the drop height. At this point, the ball + holder system is released and falls onto the sample surface. The vertical guides ensured that the ball always impacted at the same location on the sample surface. A total of 1000 impacts were performed at a frequency of 45 impacts/min, using a drop height of 90 mm. The surfaces and polished cross-section of the tested samples were inspected by SEM and optical microscopy.

The single splats were observed by SEM and sectioned in situ by focused ion beam (FIB) technique, using a dual beam machine (StrataTM DB235, FEI) combining a high-resolution FIB column and a Field Emission-SEM

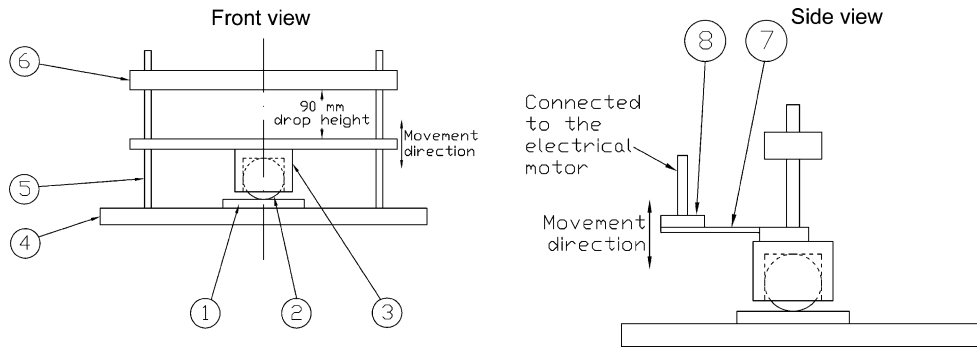

Fig. 1 Schematic diagram of the cyclic impact test equipment. Legend: 1 = sample; 2 = steel ball; 3 = ball holder; 4 = base (the sample is clamped to the base, not shown in the diagram); 5 = vertical guide for the ball holder; 6 = horizontal bar (defines the drop height); 7 = magnetic steel block; 8 = permanent magnet (attached to an electric motor through a crank-rod system, not shown in the diagram)

column. Sections were produced using an ion beam current of 7 nA and polished using an ion beam current of 300 pA.

The corrosion behavior of all coatings was tested by electrochemical impedance spectroscopy (EIS) and by open circuit potential (OCP) recording, in contact with a 3.5% NaCl aqueous solution. In EIS tests, an exposed surface of 1 cm^2 was employed; the reference electrode was $Ag/AgCl/KCl_{(sat.)}$ and the counter electrode was a Pt grid. The tests, which scanned a 100 kHz to 3 mHz frequency range (8 points/decade), were performed using an Ametek VersaStat3 potentiostat (Princeton Applied Research), with voltage perturbation amplitude of ±10 mV around OCP for WC-CoCr and of ±100 mV around OCP for anodized films. Tests were started with a 30 min delay. The OCP was recorded against Ag/AgCl reference electrodes over a 1 week period; the exposed sample surface was ≈7 cm^2, in contact with ≈200 cm^3 of test solution. The tested samples were observed by optical microscope and by SEM. The chemical composition of the test solutions was analyzed by Inductively Coupled Plasma-Atomic Emission Spectrometry (ICP, Liberty-Varian 500).

3. Results and Discussion

3.1 Microstructural, Mechanical, and Tribological Properties

The porosity of the cermet coatings decreases remarkably as the number of torch scans increases (Fig. 2, Table 2). To explain such trend in coating porosity, the coating deposition mechanism should be considered.

HVOF-sprayed cermet particles impinging onto the substrate possess very high velocity and are in a semisolid state (Ref 13); indeed, their temperatures are typically well below the melting point of WC, and they can sometimes be so low that even the CoCr matrix may be partly unmelted (Ref 14). The resulting impact pressure is large enough to deform a soft substrate (as an Al alloy) extensively (Fig. 3a), whereas this does not occur with harder substrates like steels (Fig. 3b).

In the latter case, most of the kinetic energy of the particle can therefore be employed to deform the particle itself, so that well-flattened lamellae containing few internal defects are produced. These lamellae also exhibit significant splashing. It is known that when the momentum versus viscosity and kinetic energy versus surface tension balances (expressed by the Weber and Reynolds numbers, respectively) exceed a critical threshold (Ref 15), splashing occurs during flattening of a thermally sprayed particle. This is most probably the case for the present

Table 2 Thickness, porosity, and hardness of WC-CoCr coatings

No. of scans	Porosity, %	Thickness, μm	HV, GPa
2 scans	3.2 ± 1.1	58.6 ± 9.6	8.48 ± 2.10
3 scans	1.5 ± 0.8	79.2 ± 10.2	10.69 ± 1.92
4 scans	0.8 ± 0.2	104.4 ± 12.0	10.88 ± 1.85
5 scans	0.5 ± 0.2	136.8 ± 10.9	11.17 ± 1.58

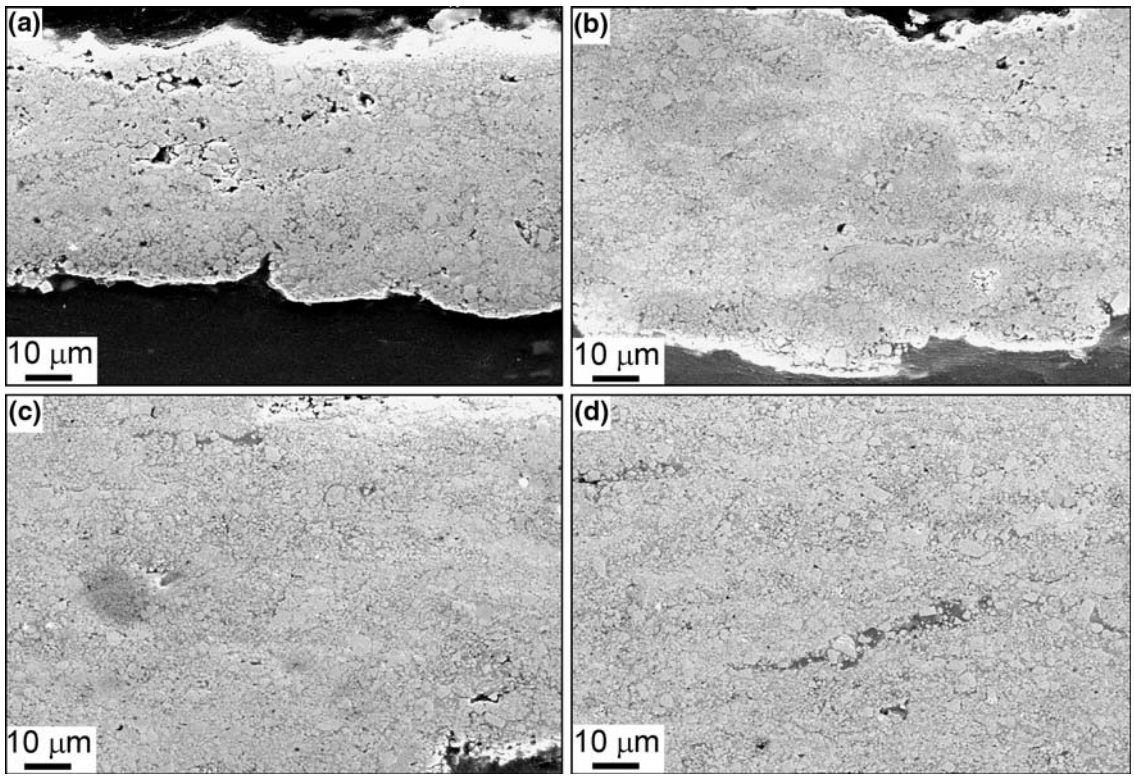

Fig. 2 Cross-sectional SEM micrographs of the WC-CoCr coatings deposited using 2 (a), 3 (b), 4 (c), and 5 (d) torch scans

HVOF-sprayed WC-CoCr particles, as they possess high density and velocity in excess of 500 m/s (Ref 16).

In contrast, the extensive deformation of the Al substrate causes the particles to penetrate deep into its surface (Fig. 3a), as also previously shown in Ref 17. These particles cannot spread and flatten, also because most of the energy is dissipated in deforming the substrate itself; consequently, the lamellae retain significant internal porosity (Fig. 3c). The very first cermet layers sprayed onto a soft substrate are therefore somewhat porous.

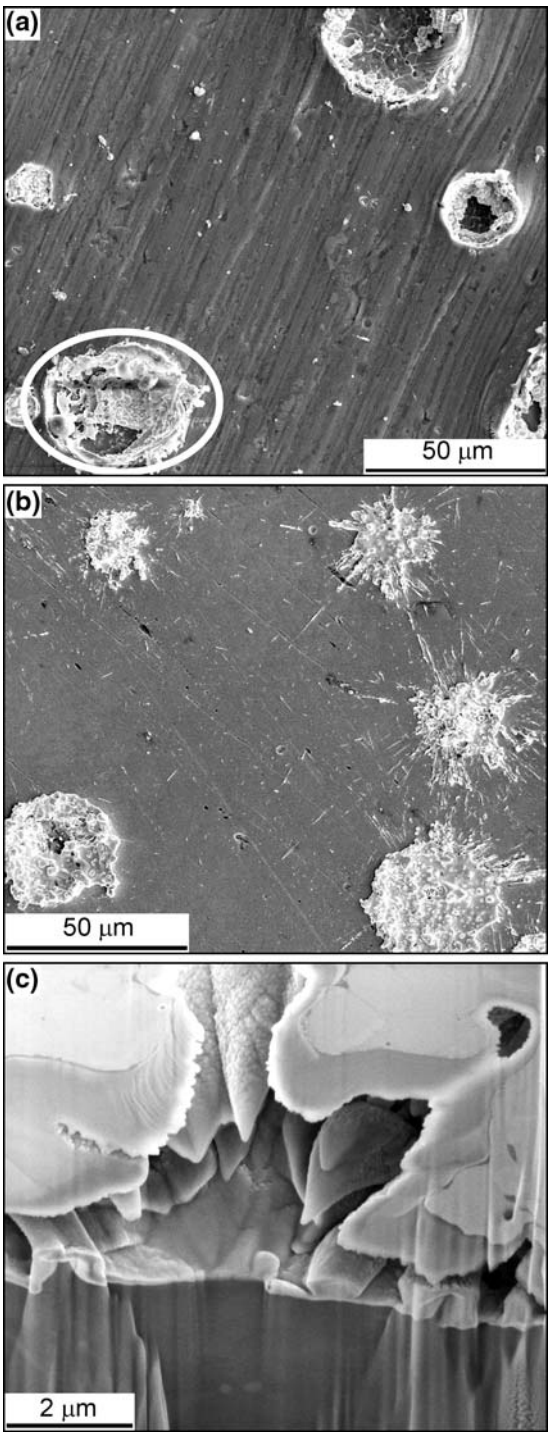

Fig. 3 SEM micrographs of the WC-CoCr single splats deposited onto ground Al (a) and steel (b) surfaces and of a FIB section produced in the splat marked by a circle in panel a (c), viewed at an angle of 52°

The coating densification at increasingly large numbers of torch scans can be explained, first of all, by the peening action (Ref 17, 18) experienced by previously deposited layers as new WC-CoCr particles impact on them. Such peening also improves the adhesion of the first layer to its substrate. If this was the only densification mechanism, however, a porosity gradient should exist across the cross-section of the thicker coatings, as their topmost layer has not been peened, but this is not the case (Fig. 2). A second factor should be considered: whereas the deposition of the first coating layers is affected by the low substrate hardness, the new incoming particles encounter a much harder surface, once a sufficiently large number of torch scans has been performed. These latter particles can therefore spread and flatten after impact, similar to the single splats collected on steel. Consequently, the resulting lamellae do not retain internal porosity.

The coating densification results in an increase of the Vickers microhardness, confirming that the peening effect and the lower defectiveness of newly deposited layers strengthen the coating (Table 2). As hardness was measured on the polished cross-section (not on the surface), this value is not influenced by the presence of the substrate. The largest variations in hardness and porosity occur when the total number of torch scans is increased from 2 to 3. At higher number of scans, variations are less remarkable. After few torch scans, indeed, the deposited material contains much porosity, both because it bears the above-mentioned influence of the soft substrate on the particle flattening process and because it has not yet undergone a significant peening process. Its hardness is therefore much inferior to the typical values of HVOF WC-CoCr coatings (Ref 5). In contrast, after several scans, the material in the middle of the coating has undergone more peening cycles and also comes from layers which are intrinsically less defective. The measured hardness values now approach or overcome $1100HV_{0.1}$, suggesting the formation of a good-quality coating (Ref 8, 19).

The same trend is accordingly displayed by the sliding wear rate (Table 3). Specifically, the wear rates of coatings deposited with three or more torch scans are $\sim 1 \times 10^{-8}$ mm^3/Nm. This value indicates a very mild wear regime, if compared to literature data concerning cermet

Table 3 Sliding wear rate of WC-CoCr coatings and anodized layers

No. of scans	Sliding wear rate, 10^{-8} mm^3/Nm
2 scans	3.04 ± 0.49
3 scans	1.39 ± 0.16
4 scans	1.16 ± 0.42
5 scans	1.05 ± 0.18
Hard anodization	820 ± 647
Sealed anodization	Completely removed after 1000 m

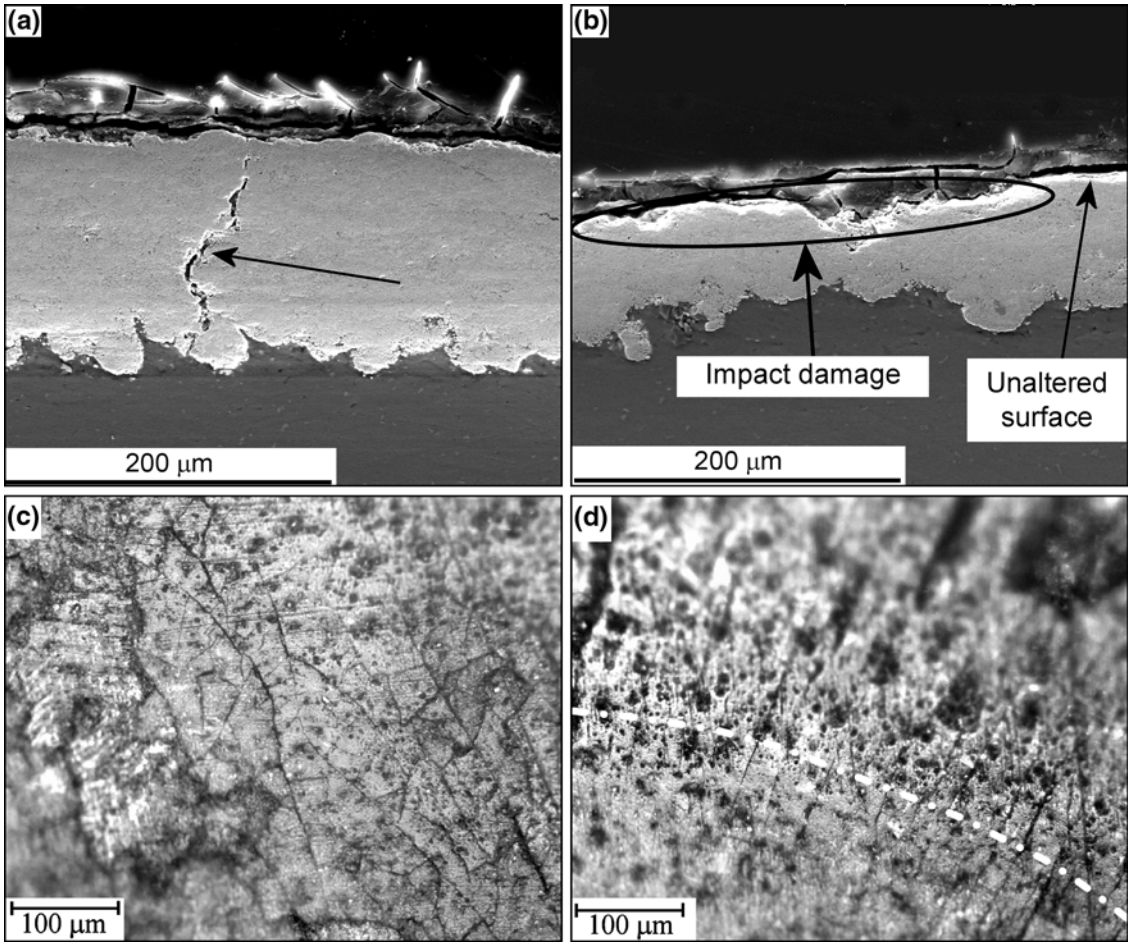

Fig. 4 Impact test results. 5-scan (a) and 2-scan (b) cermets (cross-section, SEM micrographs); hard anodized layer (surface, optical micrographs; (c) inside impact area, (d) border of impact area—see dashed line)

coatings (Ref 20). In contrast, the wear rate of the hard anodized film is higher by almost three orders of magnitude, and the sealed conventional anodized film was completely removed well before the end of the test.

The cyclic impact test indicates strong interfacial bonding between the Al substrate and the cermet coatings under localized contact conditions; indeed, the interface is free of apparent cracks, regardless of the coating thickness (Fig. 4). The overall amount of damage experienced by the thickest coatings is limited: only some limited transverse cracking (Fig. 4a, arrow) is seen. The 2-scan coating, in contrast, shows extensive near-surface damage, leading to the removal of non-negligible amounts of material (Fig. 4b, see circle). When the impact occurs, indeed, severe localized stress concentrations may arise at some asperities of the as-deposited surface and cracks may form and propagate in the near-surface region, especially if defects are present: the lower defectiveness of the coatings deposited with several torch scans can reduce the extent of such cracking, whereas the poorer cohesive strength of the 2-scan layer may result in more extensive near-surface damage.

In comparison to the WC-CoCr layers (especially to those deposited with more than 2 torch scans), the anodized films were much more severely cracked: they showed signs of delamination inside the impact area (Fig. 4c) and also displayed many radial cracks extending out of the impact area (Fig. 4d). The brittle anodized films are therefore much less compliant than the WC-CoCr cermet layers.

3.2 Corrosion Behavior

Consistent with previous studies (Ref 21, 22), the EIS spectra of the WC-CoCr coatings (Fig. 5a) exhibit two partly overlapped semicircles. These spectra were fitted using the equivalent circuit shown in Fig. 5(b), which has already been adopted for this purpose in the pertinent literature (Ref 22-24). An identical circuit has also been proposed for anodized films (Ref 25), so that direct comparison is possible between the HVOF coatings and the reference anodized films.

The first parallel R-C group (comprising the resistance R_C and the capacitance C_C) simulates the high-frequency semicircle, associated with the characteristics of the

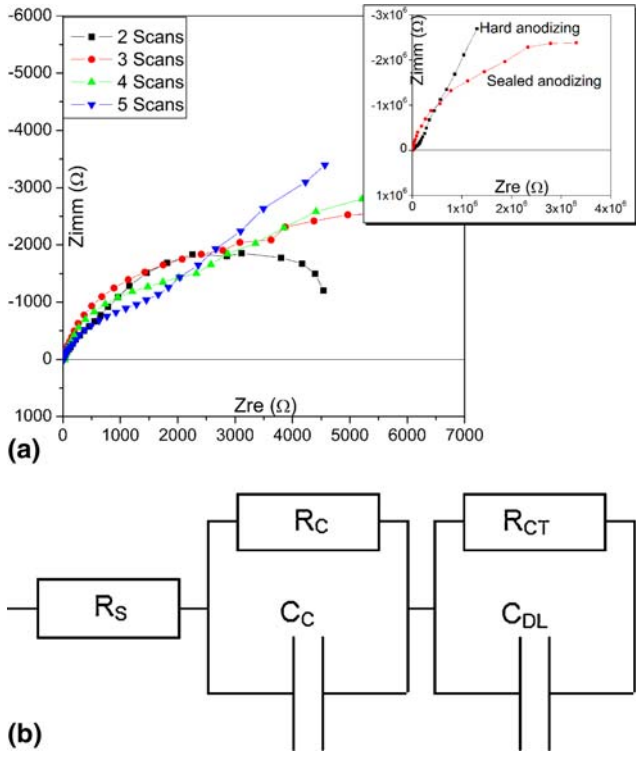

Fig. 5 EIS spectra of cermets and anodized layers (a) and equivalent circuit for spectra fitting (b)

coating layer: specifically, in cermet-coated systems, R_C and C_C are the resistance and capacitance of the cermet layer, whose open pores are filled by the electrolyte; in anodized systems, they describe the outer porous layer. The second R-C group (comprising the charge transfer resistance R_{CT} and the double layer capacitance C_{DL}) simulates the low-frequency semicircle and represents the electrolyte-electrode interface reaction: it describes the anodic dissolution of the substrate in the HVOF-coated systems, whereas, in anodized films, it is related to the dense inner barrier layer. As real (nonideal) electrochemical processes are seldom characterized by a single time constant, the double layer capacitance C_{DL} was replaced by a constant phase element Q_{DL} whose impedance is expressed as (Eq 1):

$$Z = \frac{1}{Y_{DL}(j\omega)^{n_{DL}}} \quad \text{(Eq 1)}$$

where j is the imaginary unit and $\omega = 2\pi f$, and f is the frequency.

HVOF-sprayed cermets (Table 4) exhibit a tendency toward higher R_C and R_{CT} values as the thickness of the cermet layer increases (with few exceptions), the most remarkable change occurring between the 2-scan coating and the 3-scan coating. Of all the cermet coatings, indeed, the one deposited using 2 torch scans is the thinnest and most porous. Many interconnected paths between the top surface and the substrate interface therefore exist, making the resistance against electrolyte penetration in the coating (R_C) low and the anodic dissolution of the substrate

Table 4 Average values from EIS spectra fitting

	R_S, Ω	R_C, Ω	C_C, μF	R_{CT}, Ω	Y_{DL}, $\mu S * s^{n_{DL}}$	n_{DL}
2 scans	15.6	168	518	5,520	39.7	0.73
3 scans	17.3	995	292	10,800	33.1	0.70
4 scans	28.5	1180	245	10,770	31.2	0.67
5 scans	32.2	1308	277	13,710	39.3	0.66
4 scans OCP −100 mV	21.5	1093	235	8,760	11.3	0.59
4 scans OCP +100 mV	17.2	1183	213	6,180	6.84	0.58

easy (low R_{CT}). The increase in thickness and the remarkable decrease in porosity when performing one more torch scan clearly improve the coating protectiveness. As the number of scans is increased further, improvements still occur, both because the coating is progressively densified and because interconnected paths in thick coatings become increasingly long and tortuous, but they are not as remarkable as that from 2 to 3 scans.

To verify that the above-described physical meaning of the equivalent circuit's elements is correct, further EIS tests were performed on the 4-scan cermet coating while applying base overpotentials of −100 mV and +100 mV versus OCP. These overpotentials speed up either the cathodic or the anodic reaction, respectively; therefore, they modify the overall rate of the electrochemical reaction. If the physical interpretation of the equivalent circuit's elements is correct, the values of R_{CT}, Y_{DL}, and n_{DL} should change, as they depend on that electrochemical reaction, whereas R_C and C_C should be unaffected, as they depend on the coating's thickness and porosity and not on electrochemical reactions. The results obtained by EIS spectra fitting confirm these expectations (Table 4), thus corroborating to the previous assumptions.

EIS measurements therefore indicated that, in HVOF-coated systems, the Al substrate is anodically dissolved by the electrolyte penetrating the porosity of the cermet coating; therefore, the system's OCP depends on the ratio between the area of the anodic region (the portions of the substrate exposed to the electrolyte by interconnected pores) and the area of the cathodic region (the nobler coating): the lowest the anodic/cathodic area ratio, the highest is the OCP (Ref 21). At the beginning of the test, all of the cermet coatings are rapidly infiltrated by the electrolyte; therefore, all OCP values are within the −400 to −450 mV range (Fig. 6), but the thicker and denser 5-scan coating (which possesses less interconnected porosity) is nobler than the thin, porous 2-scan coating (which possesses more interconnected porosity). If no interconnected paths had existed between the surface of the coating and the substrate, the OCP, which would have reflected the electrochemical characteristics of the cermet layer alone, would have been nobler than the currently recorded values (Ref 21).

During the 7 day test, the anode/cathode area ratio of the thickest coatings (4 and 5 scans) seems not to increase; it rather decreases slightly, as the OCP increases up to ≈−300 mV. Presumably, the cermet coating is not significantly affected by the NaCl solution, so that interconnected paths are not enlarged during the test. Accordingly,

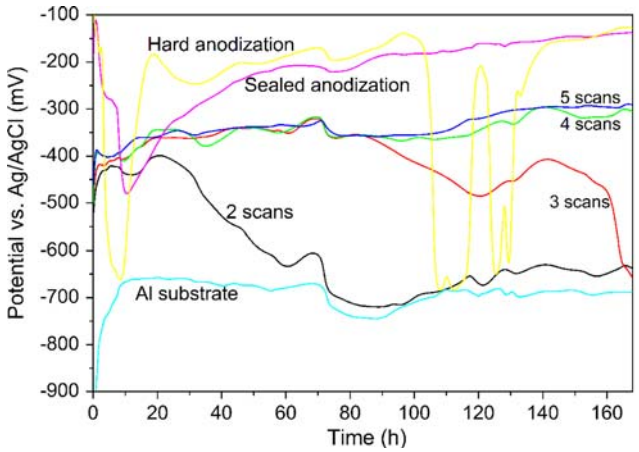

Fig. 6 Open circuit potential evolution over a 1 week period

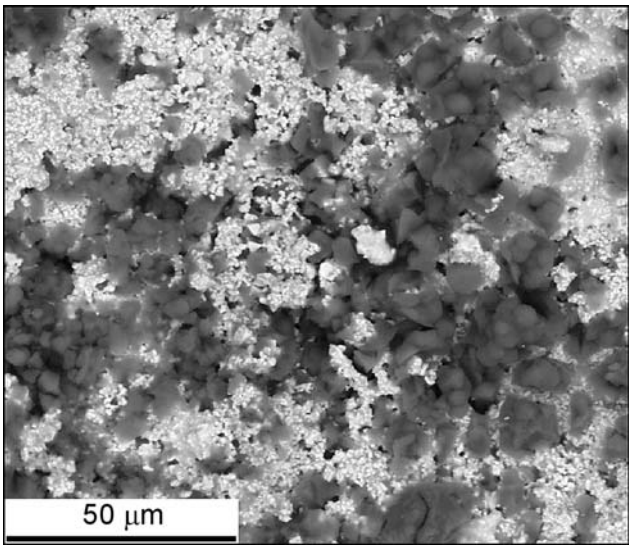

Fig. 7 SEM micrograph of the 5-scan cermet coating after the 1 week OCP monitoring test

no significant alteration of WC-CoCr cermets was noted even after long-term corrosion tests in 0.5 M H_2SO_4, unless large anodic overpotentials are applied (Ref 4). Moreover, as some anodic dissolution of the substrate occurs, corrosion products (showing a dark contrast in backscattered electron micrographs) containing Al and Cl (according to EDX microanalysis) emerge on top of these thick coatings (Fig. 7): presumably, the precipitation of these products on top of the coating surface obstructs the underlying interconnected pores and hinders further access of the corrosive solution.

This latter finding is somewhat in disagreement with the results reported in previous studies dealing with WC-CoCr coatings on steel substrates (Ref 26-28). These coatings, indeed, were found to undergo general corrosion after exposure to artificial seawater (an electrolyte which is quite similar to the 3.5% NaCl solution). A recent report on WC-CoCr coatings deposited on an Al alloy substrate and exposed to 0.5 M H_2SO_4 also showed the formation of pseudopassive films consisting of oxides and hydroxides of W and Co, without any perceivable corrosion of the substrate (Ref 4).

Compared to the WC-CoCr/steel systems, the galvanic effects between the Al substrate and the cermet layer are probably much more relevant (as Al is much less noble than steel); moreover, the currently considered cermet coatings are thinner than in the papers mentioned above (Ref 26-28). Analogously, the cermet coatings described in Ref 4 were deposited onto a thick Ni-5%Al bond coat: not only does the bond coat interrupt the possible interconnected paths between the cermet top layer and the substrate but it also offers a harder surface, preventing the formation of pores in the first cermet layers (as described in Sect. 3.1), so that the coating deposition mechanism in Ref 4 are quite different from the present ones. Selective anodic dissolution of the substrate is therefore remarkably enhanced in this case, with the coating acting as the cathode.

Accordingly, gas bubbles are seen on the surface of the 5-scan cermet coating during the OCP monitoring test (photograph in Fig. 8a): they are probably due to H_2 evolution on and inside the coating, which acts as the cathode. Previous studies have indeed suggested that the most likely cathodic process occurring on cermet-coated systems is H_2 evolution, rather than O_2 reduction (Ref 4, 22).

As the interconnected paths in the 4- and 5-scan cermet coating are narrow and tortuous, the corrosion products emerging from them (Fig. 7) cannot be observed visually (photograph in Fig. 8a).

The thinner coatings (2- and 3-scans) also display a trend toward slightly increasing OCP during the first stages of the test, but, later on, the OCP starts decreasing very remarkably, achieving a final value of about −700 mV (Fig. 6), i.e., close to the OCP of the bare Al substrate. As the OCP starts decreasing, white corrosion products become visible at some spots on the coatings' top surface (Fig. 8b). As the test progresses, the number of localized areas showing white corrosion products increases (Fig. 8c, see arrows). Simultaneously, many more gas bubbles appear: this indicates a definite acceleration in the cathodic reaction (H_2 evolution), witnessing an increase in the overall rate of the electrochemical corrosion reaction.

As explained previously, the thinner coatings have more interconnected pores; moreover, due to the roughness of the substrate interface, their thickness can be very low in some points. Because of the stochastic nature of the thermal spray process, some more defective areas can also be randomly distributed in the coating, as previously noted for HVOF-sprayed cermets on Mg alloys (Ref 10). Consequently, there are some definite locations on the samples where the electrolyte can reach the Al substrate very easily. In those locations, the anodic dissolution of the substrate is particularly fast, so that a very large amount of corrosion products accumulates along the coating/substrate interface and detaches the coating, lifting it off the substrate surface (Fig. 9). The corrosion products can therefore emerge to the sample surface,

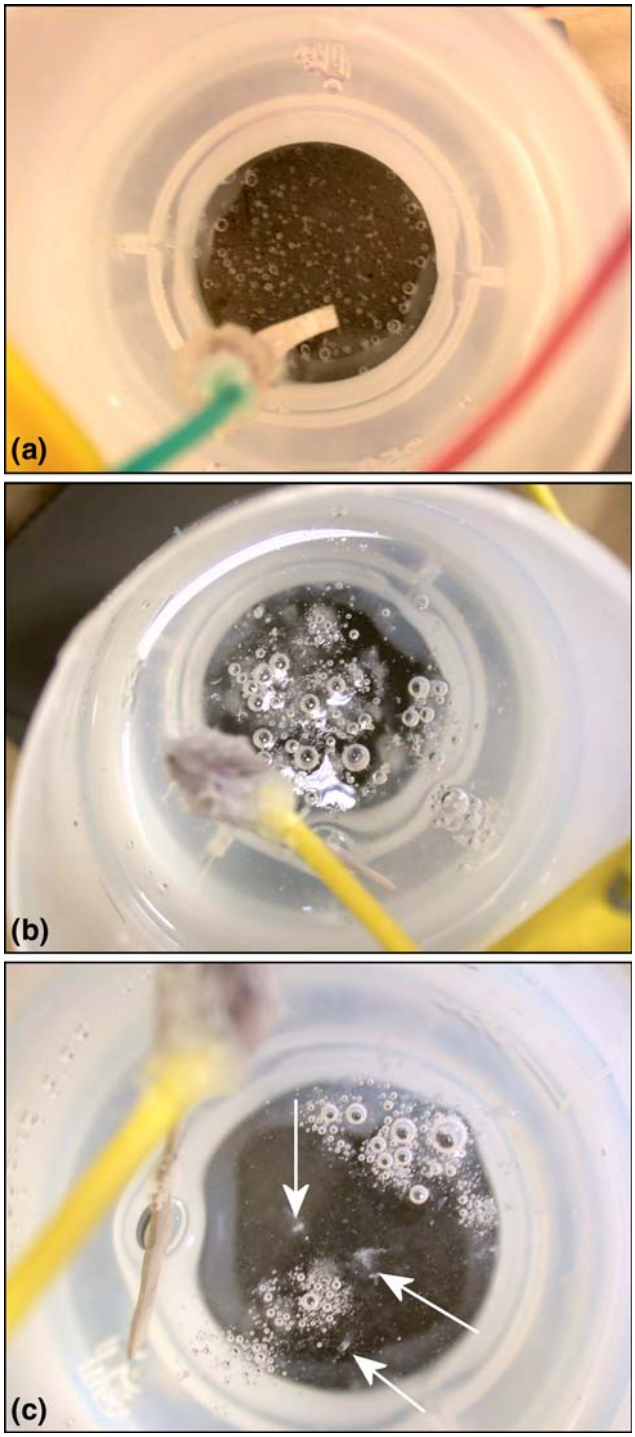

Fig. 8 Digital photographs of cermet-coated systems during the OCP monitoring test: 5-scan coating after 7 days (a); 2-scan coating after 2 days (b); and 2-scan coating after 3 days (c). The arrows indicate some corrosion spots

giving rise to the ''white spots'' visually noticeable in Fig. 8(b) and (c).

When the coating is spalled, it cannot exert any protective action toward the substrate, which can be directly accessed by the electrolyte, so that the potential drops to

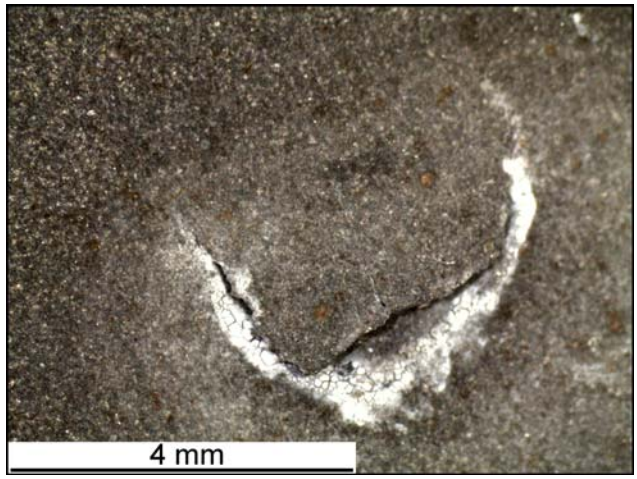

Fig. 9 Stereomicroscopic view of a spalled region on the 2-scan coating at the end of the OCP monitoring test

−700 mV. Under these conditions, the presence of the coating even turns out to be detrimental; indeed, the overall amount of Al dissolved into the NaCl solution at the end of the 7 day test performed on the 2-scan coating is 187 μg/cm^2, whereas the amount of Al released by the bare Al substrate is 27 μg/cm^2. This is explained by the severe galvanic corrosion occurring on the exposed substrate while the surrounding coating acts as a cathode. When the 4- and 5-scan coatings are considered, instead, the amount of dissolved Al is only around 10 μg/cm^2.

The corrosion protectiveness of all of the cermet coatings, however, compares unfavorably to the anodized films. There is indeed a difference of one or more orders of magnitude between the EIS responses of HVOF-sprayed cermets and of anodized films (Fig. 5b, Table 4). Consistently, the OCP of the sealed anodized films, after an initial transitory phase, attains a quite high value, increasing up to ≈−140 mV at the end of the 7 day period. The hard anodized film shows some sudden drops in the OCP down to about −700 mV, but eventually attains a value of about ≈−140 mV as well. Perhaps, the outer layer of the hard anodized film, which did not undergo any sealing treatment, contains a few pores which allow the electrolyte to slowly penetrate and reach the barrier layer. Although such layer is very dense, it can be locally attacked by the NaCl solution, as chlorides can chemically alter Al_2O_3-based films. When the solution damages the barrier layer, the OCP drops. In this case, however, no galvanic effect accelerates the corrosion of the substrate; minor amounts of corrosion products precipitating inside the defects can therefore heal the film, thus restoring the high OCP value.

The amount of Al dissolved into the electrolyte by both anodized films at the end of the test is about 5 μg/cm^2, i.e., one half of the value recorded for the best cermet coatings. This confirms the superior protectiveness of anodized films, particularly when it is considered that some of that dissolved Al might even come from the film itself, not from substrate corrosion.

4. Conclusions

The number of scans performed by the HVOF torch to deposit WC-CoCr cermet coatings onto Al alloy substrates has a major influence on the coatings' characteristics. Apart from the obvious variation in thickness, their microstructure also changes because of a modification in the deposition mechanisms.

The kinetic energy of cermet particles directly impacting onto the soft Al surface is indeed dissipated by the deformation of the surface itself: the particles do not flatten properly and generate significant defectiveness. Thin layers (deposited using few torch cycles) are therefore quite porous; instead, thicker ones, deposited by performing several torch scans, are denser, because of two reasons. First, the high-velocity impact of new particles peens the previously deposited cermet layers and densifies them and second, the new particles can flatten more efficiently, as they impact on a much harder surface (the previously deposited coating layers).

On account of such densification, the hardness of the coating improves, the sliding wear rate decreases, and the protectiveness against substrate corrosion is enhanced. In particular, the largest differences exist between the coatings deposited using 2- and 3-torch scans: when the number of torch scans is low, the densification effects obtained by performing an additional torch scan are the most remarkable; further improvements become less important.

A detail examination of the coatings' performances in comparison to those of anodized films indicates that HVOF-sprayed WC-CoCr is definitely preferable in applications where wear-resistance is required, as the dry sliding wear rate of the cermet coatings is lower than that of a hard anodized film by several orders of magnitude. Three torch scans seem to be enough to confer excellent wear resistance (close to 1×10^{-8} mm^3/Nm) to the WC-CoCr coating. In contrast, even the thickest HVOF-sprayed WC-CoCr coating tested in this study is far less protective than anodized films against substrate corrosion in a 3.5% NaCl solution. It seems that all of the present cermet coatings have a certain degree of interconnected porosity, allowing the solution to reach the coating interface. Consequently, the substrate is anodically dissolved while the coating acts as the cathode. Moreover, thin cermet layers can also contain some highly defective spots, where the preferential anodic dissolution of the substrate is particularly accelerated. The coating can therefore be locally detached because of the accumulation of corrosion products along the interface. Under these circumstances, the overall corrosion damage experienced by the substrate is even larger than that undergone by bare Al.

Acknowledgments

The authors wish to acknowledge the production of the HVOF-sprayed cermet coatings by Ing. Fabrizio Casadei, Mr. Francesco Barulli, Mr. Edoardo Severini, and Mr. Carlo Costa, Centro Sviluppo Materiali S.p.A., Roma, Italy. Thanks to Dr. Roberto Giovanardi for the assistance with corrosion testing and to Dr. Maria Cannio for the ICP analyses. We are grateful to Mr. Fabio Pighetti Mantini and to Ing. Andrea Bassani for their assistance with part of the experimental activity. We also acknowledge Dr. Enrico Gualtieri for providing the SEM micrographs and FIB sections of single splats. Thanks to Mr. Gadda (Mochem s.r.l., Modena, Italy) for performing the anodization treatments. This study was partly supported by PRRIITT (Regione Emilia-Romagna), Net-Lab ''Surface & Coatings for Advanced Mechanics and Nanomechanics'' (SUP&RMAN).

References

1. M.F. Ashby, Y.J.M. Bréchet, D. Cebon, and L. Salvo, Selection Strategies for Materials and Processes, *Mater. Des.*, 2004, **25**, p 51-67
2. B. Wielage, A. Wank, H. Pokhmurska, T. Grund, C. Rupprecht, G. Reisel, and E. Friesen, Development and trends in HVOF spraying technology, *Surf. Coat. Technol.*, 2006, **201**, p 2032-2037
3. H. Takahashi, Aluminum Anodizing, Corrosion: Fundamentals, Testing, and Protection, *ASM Handbook*, Vol 13A, ASM International, Materials Park, OH, 2003, p 736-740
4. A. Lekatou, E. Regoutas, and A.E. Karantzalis, Corrosion Behaviour of Cermet-Based Coatings with a Bond Coat in 0.5 M H_2SO_4, *Corros. Sci.*, 2008, **50**, p 3389-3400
5. P.G. Sheasby and R. Pinner, *The Surface Treatment and Finishing of Aluminum and Its Alloys*, ASM International/Finishing Publications Ltd, Materials Park, OH/Stevenage, UK, 2001
6. I. Tsangaraki-Kaplanoglou, S. Theohari, T. Dimogerontakis, Y.-M. Wang, H.-H. Kuo, and S. Kia, Effect of Alloy Types on the Anodizing Process of Aluminum, *Surf. Coat. Technol.*, 2006, **200**, p 2634-2641
7. D.E. Crawmer, Thermal Spray Processes, *Handbook of Thermal spray Technology*, J.R. Davis, Ed., ASM International, Materials Park, OH, 2004, p 54-84
8. A. Wank, B. Wielage, H. Pokhmurska, E. Friesen, and G. Reisel, Comparison of Hardmetal and Hard Chromium Coatings Under Different Tribological Conditions, *Surf. Coat. Technol.*, 2006, **201**, p 1975-1980
9. G. Bolelli, R. Giovanardi, L. Lusvarghi, and T. Manfredini, Corrosion Resistance of HVOF-Sprayed Coatings for Hard Chrome Replacement, *Corros. Sci.*, 2006, **48**, p 3375-3397
10. M. Parco, L. Zhao, J. Zwick, K. Bobzin, and E. Lugscheider, Investigation of HVOF Spraying on Magnesium Alloys, *Surf. Coat. Technol.*, 2006, **201**, p 3269-3274
11. G.J. Gibbons and R.G. Hansell, Down-Selection and Optimization of Thermal-Sprayed Coatings for Aluminum Mould Tool Protection and Upgrade, *J. Therm. Spray Technol.*, 2006, **15**, p 340-347
12. M. Magnani, P.H. Suegama, N. Espallargas, S. Dosta, C.S. Fugivara, J.M. Guilemany, and A.V. Benedetti, Influence of HVOF Parameters on the Corrosion and Wear Resistance of WC-Co Coatings Sprayed on AA7050 T7, *Surf. Coat. Technol.*, 2008, **202**, p 4746-4757
13. Y.-Y. Wang, C.-J. Li, and A. Ohmori, Examination of Factors Influencing the Bond Strength of High Velocity Oxy-Fuel Sprayed Coatings, *Surf. Coat. Technol.*, 2006, **200**, p 2923-2928
14. S. Kamnis, S. Gu, T.J. Lu, and C. Chen, Computational Simulation of Thermally Sprayed WC-Co Powder, *Comput. Mater. Sci.*, 2008, **43**, p 1172-1182
15. M. Fukumoto, E. Nishioka, and T. Nishiyama, New Criterion for Splashing in Flattening of Thermal Sprayed Particles onto Flat Substrate Surface, *Surf. Coat.Technol.*, 2002, **161**(2-3), p 103-110
16. W. Trompetter, M. Hyland, D. McGrouther, P. Munroe, and A. Markwitz, Effect of Substrate Hardness on Splat Morphology in High-Velocity Thermal Spray Coatings, *J. Therm. Spray Technol.*, 2006, **15**, p 663-669

17. S. Kuroda, Y. Tashiro, H. Yumoto, S. Taira, H. Fukanuma, and S. Tobe, Peening Action and Residual Stresses in High-Velocity Oxygen Fuel Thermal Spraying of 316L Stainless Steel, *J. Therm. Spray Technol.*, 2001, **10**, p 367-374
18. P. Bansal, P.H. Shipway, and S.B. Leen, Effect of Particle Impact on Residual Stress Development in HVOF Sprayed Coatings, *J. Therm. Spray Technol.*, 2006, **15**, p 570-575
19. J. Barber, B.G. Mellor, and R.J.K. Wood, The Development of Sub-Surface Damage During High Energy Solid Particle Erosion of a Thermally Sprayed WC-Co-Cr Coating, *Wear*, 2005, **259**, p 125-134
20. Q. Yang, T. Senda, and A. Ohmori, Effect of Carbide Grain Size on Microstructure and Sliding Wear Behaviour of HVOF-Sprayed WC-12%Co Coatings, *Wear*, 2003, **254**, p 23-34
21. A. Collazo, X.R. Nóvoa, and C. Pérez, Corrosion Behaviour of Cermet Coatings in Artificial Seawater, *Electrochim. Acta*, 1999, **44**, p 4289-4296
22. P.H. Suegama, C.S. Fugivara, A.V. Benedetti, J.M. Guilemany, J. Fernández, and J. Delgado, The Influence of Gun Transverse Speed on Electrochemical Behaviour of Thermally Sprayed Cr_3C_2-NiCr Coatings in 0.5 M H_2SO_4 Solution, *Electrochim. Acta*, 2004, **49**, p 627-634
23. J.M. Guilemany, J. Fernández, J. Delgado, A.V. Benedetti, and F. Climent, Effects of Thickness Coating on the Electrochemical Behaviour of Thermal Spray Cr_3C_2-NiCr Coatings, *Surf. Coat. Technol.*, 2002, **153**, p 107-113
24. P.H. Suegama, N. Espallargas, J.M. Guilemany, J. Fernández, and A.V. Benedetti, Electrochemical and Structural Characterization of Heat-Treated Cr_3C_2-NiCr Coatings, *J. Electrochem. Soc.*, 2006, **153**, p B434-B445
25. F. Mansfeld, Electrochemical Methods of Corrosion Testing, Corrosion: Fundamentals, Testing, and Protection, *ASM Handbook*, Vol 13A, ASM International, Materials Park, OH, 2003, p 446-462
26. C. Monticelli, A. Frignani, and F. Zucchi, Investigation on the Corrosion Process of Carbon Steel Coated by HVOF WC/Co Cermets in Neutral Solution, *Corros. Sci.*, 2004, **46**, p 1225-1237
27. A. Neville and T. Hodgkiess, Corrosion Behaviour and Microstructure of Two Thermal Spray Coatings, *Surf. Eng.*, 1996, **12**, p 303-312
28. J.E. Cho, S.Y. Hwang, and K.Y. Kim, Corrosion Behavior of Thermal Sprayed WC Cermet Coatings Having Various Metallic Binders in Strong Acidic Environment, *Surf. Coat. Technol.*, 2006, **200**, p 2653-2662